The Journal of Infectious Diseases

MAJOR ARTICLE

# Crimean-Congo Hemorrhagic Fever in Humanized Mice Reveals Glial Cells as Primary Targets of Neurological Infection

**Jessica R. Spengler,[1] M. Kelly Keating,[2] Anita K. McElroy,[1,3] Marko Zivcec,[1] JoAnn D. Coleman-McCray,[1] Jessica R. Harmon,[1] Brigid C. Bollweg,[2] Cynthia S. Goldsmith,[2] Éric Bergeron,[1] James G. Keck,[4] Sherif R. Zaki,[2] Stuart T. Nichol,[1] and Christina F. Spiropoulou[1]**

[1]Viral Special Pathogens Branch and [2]Infectious Diseases Pathology Branch, Division of High Consequence Pathogens and Pathology, Centers for Disease Control and Prevention, and [3]Division of Pediatric Infectious Diseases, Emory University, Atlanta, Georgia; and [4]In Vivo Services, The Jackson Laboratory, Sacramento, California

Crimean-Congo hemorrhagic fever (CCHF) is a tick-borne viral hemorrhagic disease seen exclusively in humans. Central nervous system (CNS) infection and neurological involvement have also been reported in CCHF. In the current study, we inoculated NSG-SGM3 mice engrafted with human hematopoietic CD34$^+$ stem cells with low-passage CCHF virus strains isolated from human patients. In humanized mice, lethal disease develops, characterized by histopathological change in the liver and brain. To date, targets of neurological infection and disease have not been investigated in CCHF. CNS disease in humanized mice was characterized by gliosis, meningitis, and meningoencephalitis, and glial cells were identified as principal targets of infection. Humanized mice represent a novel lethal model for studies of CCHF countermeasures, and CCHF-associated CNS disease. Our data suggest a role for astrocyte dysfunction in neurological disease and identify key regions of infection in the CNS for future investigations of CCHF.

**Keywords.** Crimean-Congo hemorrhagic fever; NSG-SGM3 humanized mice; neuropathology; glial cell; meningitis.

Tick-borne Crimean-Congo hemorrhagic fever virus (CCHFV; genus *Nairovirus*; family Bunyaviridae) is the etiologic agent of Crimean-Congo hemorrhagic fever (CCHF). Disease can vary from mild, nonspecific febrile illness to severe hemorrhagic clinical signs. Neurological involvement in CCHF was also described in the seminal report on the 1944 outbreak in Soviet troops in the Crimean peninsula, in which general cerebral, meningeal, and slight psychological and neurological symptoms were noted as the most characteristic clinical features in these cases [1]. Based on these findings and degeneration of the autonomic nervous system observed in later cases, CCHFV was considered by early researchers to be a neurotropic virus [2].

Further descriptions of CCHF neurological involvement and disease include a pediatric patient who presented with abnormal behavior (violent reactions, extreme agitation, and incoherent speech) and later exhibited vestibular signs [2], virus isolation from the hypothalamus in a fatal case [3], inflammatory infiltrates in the cerebrum [4], acute encephalopathy associated with subdural hematoma [5], and a fatal brain herniation [6]. Despite these findings and reports of other *Nairovirus*-associated neurological disease [7, 8], the incidence, pathogenesis, and clinical outcome of central nervous system (CNS) infection in patients with CCHF has not been investigated. In addition, in vivo model studies are limited by the absence of overt disease in animals, including nonhuman primates. Current animal models are restricted to signal transducer and activator of transcription 1 knockout (STAT-1$^{-/-}$) and interferon α/β-receptor knockout (IFNAR$^{-/-}$) mice, deficient in essential innate immune pathways [9–11].

In this article, we describe a novel lethal disease model of CCHF in humanized mice. Hu-NSG-SGM3 mice, derived from NSG-SGM3 (NOD.Cg-*Prkdc*$^{scid}$ *Il2rg*$^{tm1Wjl}$ Tg [CMV-IL3, CSF2, KITLG] 1Eav/MloySzJ) mice, are irradiated and intravenously injected with human CD34$^+$ hematopoietic stem cells. We infected SGM3 humanized mice with 2 strains of CCHFV isolated from human patients in Oman (CCHFV-OM) or Turkey (CCHFV-TR). All mice infected with CCHFV-TR developed progressive disease, with high levels of viral antigen in the liver, spleen, and brain. In mice that succumbed to disease, the highest level of virus, detected with quantitative reverse-transcription polymerase chain reaction (qRT-PCR), immunohistochemistry, and electron microscopy, was in the brain. In contrast, all mice infected with CCHFV-OM exhibited mild clinical signs and recovered; viral antigen was uniformly absent in the brains of these mice. Viral antigen was primarily detected in glial cells, including astrocytes and microglia, and in the meninges. These finding indicate that neuropathology, which included gliosis and meningitis/meningoencephalitis, is a key component of disease in this model. In addition to providing a lethal model

Received 25 March 2017; editorial decision 25 April 2017; accepted 2 May 2017; published online May 8, 2017.

Presented in part: Keystone Symposia Series: Hemorrhagic Fever Viruses, Santa Fe, New Mexico, 5 December 2016.

Correspondence: J. R. Spengler, DVM, PhD, MPH, Viral Special Pathogens Branch, Division of High Consequence Pathogens and Pathology, Centers for Disease Control and Prevention, Atlanta, GA 30333 (JSpengler@cdc.gov).

**The Journal of Infectious Diseases® 2017;216:1386–97**



DOI: 10.1093/infdis/jix215

for therapeutic studies, humanized mice can be used for further investigations of CCHF-associated neuropathogenesis in vivo.

## MATERIALS AND METHODS

### Ethics Statement

All animal procedures were approved by the Institutional Animal Care and Use Committee (2736SPEMOUC) of the Centers for Disease Control and Prevention (CDC) and conducted in accordance with the *Guide for the Care and Use of Laboratory Animals* [12]. The CDC is fully accredited by the Association for Assessment and Accreditation of Laboratory Animal Care International. Procedures conducted with CCHFV or CCHFV-infected animals were performed in the CDC biosafety level 4 laboratory.

### Humanized Mice

One donor cohort of 21 female Hu-NSG™-SGM3 mice (stock No. 701362) was obtained from Jackson Laboratories. Mice were evenly distributed in experimental groups based on the percentage of human CD45$^+$ cells in peripheral blood as determined with flow cytometry 12 weeks after engraftment. Mice were housed in a climate-controlled laboratory with a 12-hour day/12-hour night cycle, provided sterilized commercially available mouse chow and water ad libitum, and group housed with sterile bedding in an isolator caging system. Mice were humanely euthanized when clinical illness scores—based on neurological signs, changes in mentation, ataxia, dehydration, dyspnea, and/or weight loss (>20%)—indicated that the animal was in distress or in the terminal stages of disease.

### Virus Inoculation

SGM3 humanized mice (16 weeks after engraftment) were sham-injected with sterile Dulbecco's modified Eagle's medium or inoculated intraperitoneally with $10^4$ median tissue culture infective dose ($TCID_{50}$) of CCHFV Oman-199809166 (GenBank accession nos. KY362516, KY362518, and KY362514) or CCHFV Turkey-200406546 (CCHFV-TR; GenBank accession nos. KY362517, KY362519, KY362515). Both viruses were isolated from hospitalized human patients with unknown clinical outcomes. CCHFV-OM virus stock was passaged twice in Vero E6 cells and once in SW13 cells, and CCHFV-TR was passaged once in suckling mouse brain and once in SW13 cells. Inoculum titers were calculated using a method based on that of Reed and Muench [13], on SW13 cells fixed and stained with crystal violet 6 days after infection.

### qRT-PCR Methods

RNA was extracted from blood and homogenized tissue samples using the MagMAX-96 Total RNA Isolation Kit (Thermo Fisher Scientific) on a 96-well ABI MagMAX extraction platform with a DNaseI treatment step, according to the manufacturer's instructions. RNA was quantitated using a 1-step real-time RT-PCR targeting a strain-specific nucleoprotein gene sequence, and it was standardized to 18S with a SuperScript III Platinum One-Step qRT-PCR Kit (Thermo Fisher Scientific), according to the manufacturer's instructions (primer and probe sequences available on request). $TCID_{50}$ equivalents were determined by analyzing, in parallel, standard dilutions of RNA extracted from the virus stock vial used for inoculations.

### Flow Cytometry

Cell suspensions were prepared from macerated liver and spleen tissues; $2 \times 10^6$ of the spleen cells and all of the liver mononuclear cells obtained from gradient selection on Histopaque 1077 (Sigma-Aldrich) were used for subsequent flow cytometric staining. Cells were stained with LIVE/DEAD Fixable Near-IR stain (1:500) in phosphate-buffered saline, washed in flow buffer (phosphate-buffered saline, 2% fetal bovine serum) and then treated with Fc blocking reagent (Miltenyi Biotec). Surface stains were added directly to cells, and after 2 washes in flow buffer, cells were treated with Fix/Perm and then washed twice in Perm/Wash buffer (both from BD). Intracellular staining was done for perforin-PCP-Cy5.5 (delta G9; BD), followed by 2 washes in Perm/Wash buffer before data were acquired on a Stratedigm cytometer. Data were analyzed using FlowJo software, version 10 (Tree Star). Three of the 5 CCHFV-TR mice with terminal-stage disease were excluded because flow cytometry could not be performed in real time on the day of euthanasia. One mouse was excluded from flow cytometric analyses owing to low engraftment (mouse OM-7; 12% CD45$^+$ cells in liver and spleen). For additional details on tissue processing, cell staining, and antibody panels see Supplementary Methods.

### Histochemical Staining, Immunohistochemistry, and Electron Microscopy

Tissue specimens were fixed in 10% neutral buffered formalin and subjected to gamma irradiation ($2 \times 10^6$ rad). Tissues were routinely processed for paraffin embedding, sectioning and staining with hematoxylin-eosin, and select samples were stained with Prussian blue for detection of iron. For immunohistochemical assays, slides were stained with a rabbit polyclonal antibody reactive to CCHFV N protein (IBT Bioservices) diluted 1:1000 and/or glial fibrillary acidic protein 6F2 (Agilent Technologies) diluted 1:200. On-slide embedding and transmission electron microscopy were performed as described elsewhere [14]. Areas were selected that, in a serial light microscopic section, had shown intense anti-CCHFV immunoreactivity. For additional details on slide processing, see Supplementary Methods.

## RESULTS

### CCHFV Replication and Dissemination in SGM3 Humanized Mice

SGM3 humanized mice were inoculated intraperitoneally with $10^4$ $TCID_{50}$ of CCHFV-OM (n = 9) or CCHFV-TR (n = 8) strains. Three mice per group, and a control, were euthanized 4 days after infection to assess clinical chemistry findings (Supplementary Figure S1), and viral replication early in

infection. The other animals were followed up clinically and sampled as described above, after euthanasia due to disease or at study completion (33 days after infection). Animals inoculated with CCHFV-OM (n = 6) exhibited minimal weight loss and recovered (maximum median loss at 2 days after infection, 4.99% ± 4.47% SD; maximum absolute loss at 3 days after infection, 16.7%; Figure 1A). In contrast, animals inoculated with CCHFV-TR (n = 5) displayed slow progressive weight loss, ultimately requiring euthanasia at 13, 20, or 23 days after infection (Figure 1B). Viral RNA levels were determined by qRT-PCR in blood and tissues of CCHFV-inoculated SGM3 humanized mice (Figure 1C).

At 4 days after infection, viral RNA was detected in all blood and tissue samples analyzed from mice infected with

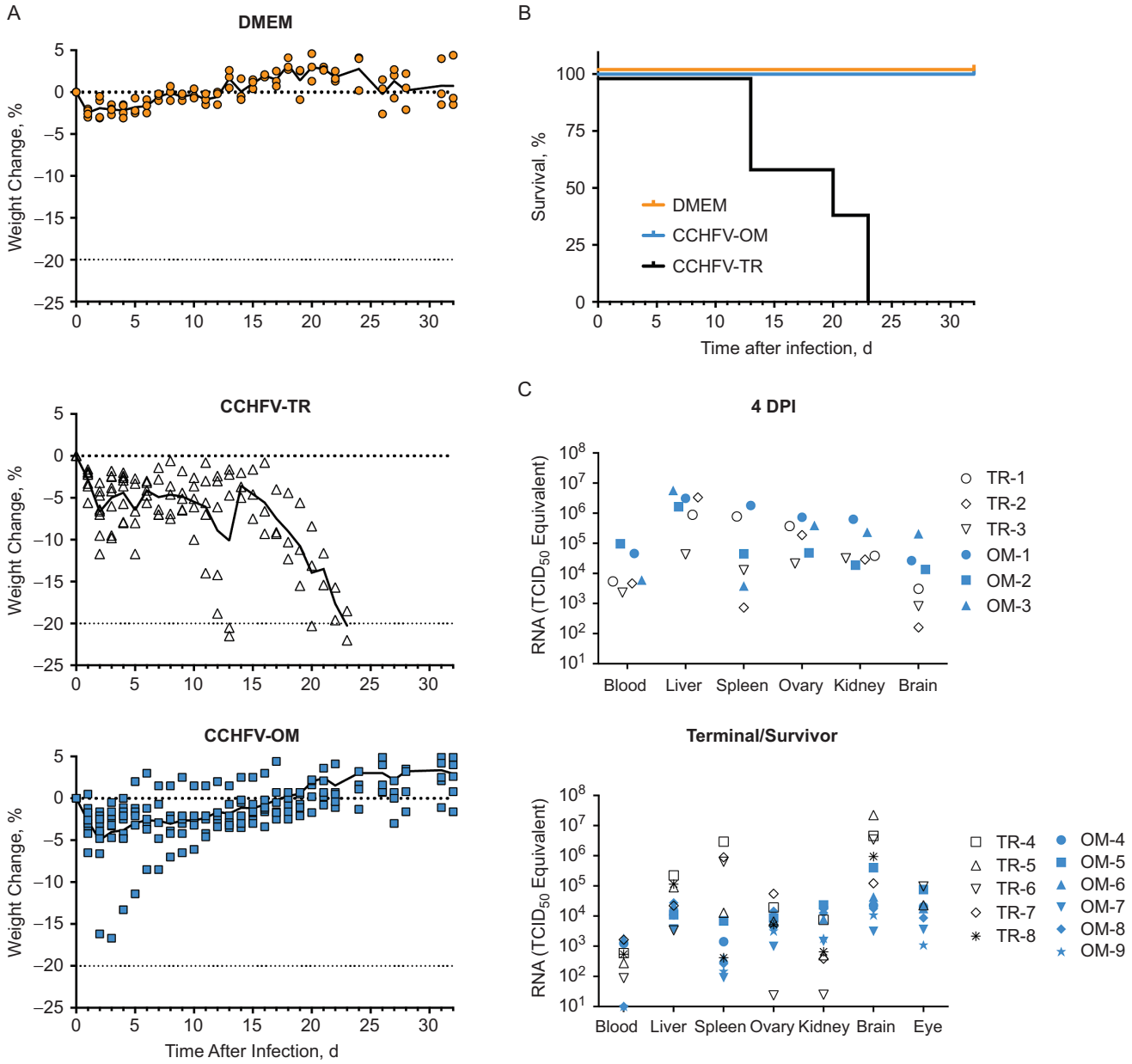


**Figure 1.** Weight loss, survival and RNA loads in blood and tissues of SGM3 humanized mice inoculated with a Crimean-Congo hemorrhagic fever virus strain isolated from a human patient in Oman (CCHFV-OM) or Turkey (CCHFV-TR). *A,* Weight change in $CD34^+$ engrafted humanized mice inoculated intraperitoneally with Dulbecco's modified Eagle's medium (DMEM) (mock), or with $10^4$ median tissue culture infective dose ($TCID_{50}$) of CCHFV-OM or CCHFV-TR. Symbols represent each individual animal sampled at that time point; lines represent mean weight change for all individuals on that day. On days 1–4 after infection, all animals inoculated are represented (DMEM, n = 4; CCHFV-OM, n = 9; CCHFV-TR, n = 8). Animals euthanized for early infection sampling are absent in the remainder of the sampling days (remaining DMEM, n = 3; OM, n = 6; TR, n = 5). *B,* Survival in humanized mice inoculated intraperitoneally with DMEM (n = 3), or with $10^4$ $TCID_{50}$ of CCHFV (OM, n = 6; TR, n = 5). *C,* Viral RNA quantitation at 4 days after infection, time when the animal met euthanasia criteria (terminal), or study completion (33 days after infection, survivor) in mice inoculated with CCHFV-TR (*black-and-white symbols*) and CCHFV-OM (*blue symbols*). Quantitative reverse-transcription polymerase chain reaction was performed based on primer-probes specific for the nucleoprotein of each strain, and $TCID_{50}$ equivalents were calculated based on standards generated from inoculum virus.

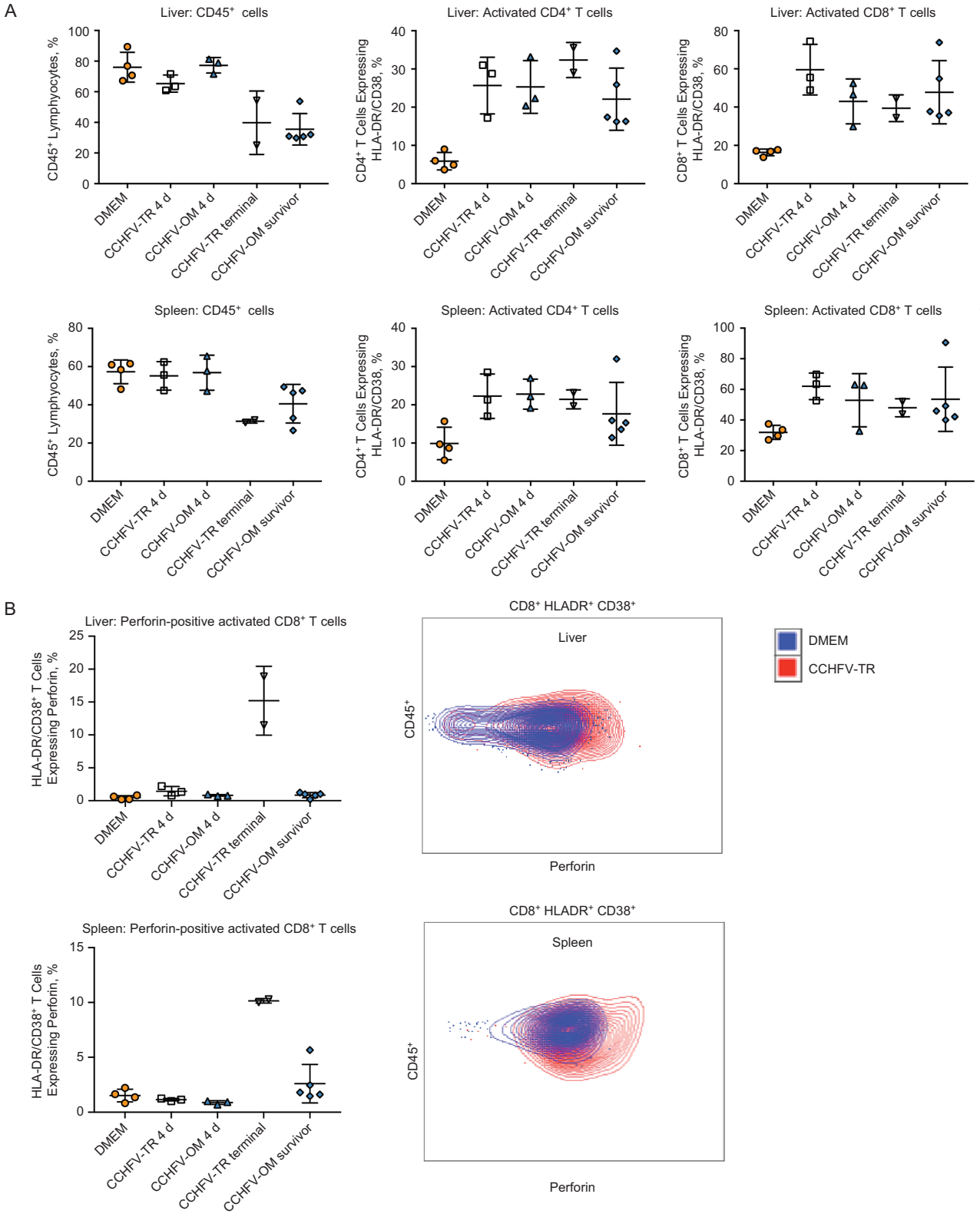


**Figure 2.** Characterization of human CD45+ cell reconstitution, T-cell activation, and CD8+ T-cell perforin expression in liver and spleen tissue from SGM3 humanized mice infected with Crimean-Congo hemorrhagic fever virus (CCHFV). *A,* Quantitation of human CD45+ cells in liver and spleen demonstrates decreased lymphocyte populations at late time points in infected animals, independent of viral strain or presence of disease. Both CD4+ and CD8+ T cells were found to be activated in mice infected with CCHFV, at early and late time points, independent of viral strain or presence of disease. CCHFV-OM and TR, CCHFV isolated from human patients in Oman and Turkey, respectively; DMEM, Dulbecco's modified Eagle's medium; 4 d, 4 days after infection. *B,* Flow cytometric analysis of perforin expression in liver and spleen samples from mock and CCHFV-infected SGM3 humanized mice. Data are presented as percentage of HLA-DR/CD38+ T cells expressing perforin (with standard deviation), and representative contour plots demonstrate shift in expression observed in mice with terminal-stage disease infected with a CCHFV-TR (*red*) compared with control mice sham-infected with DMEM (*blue*).

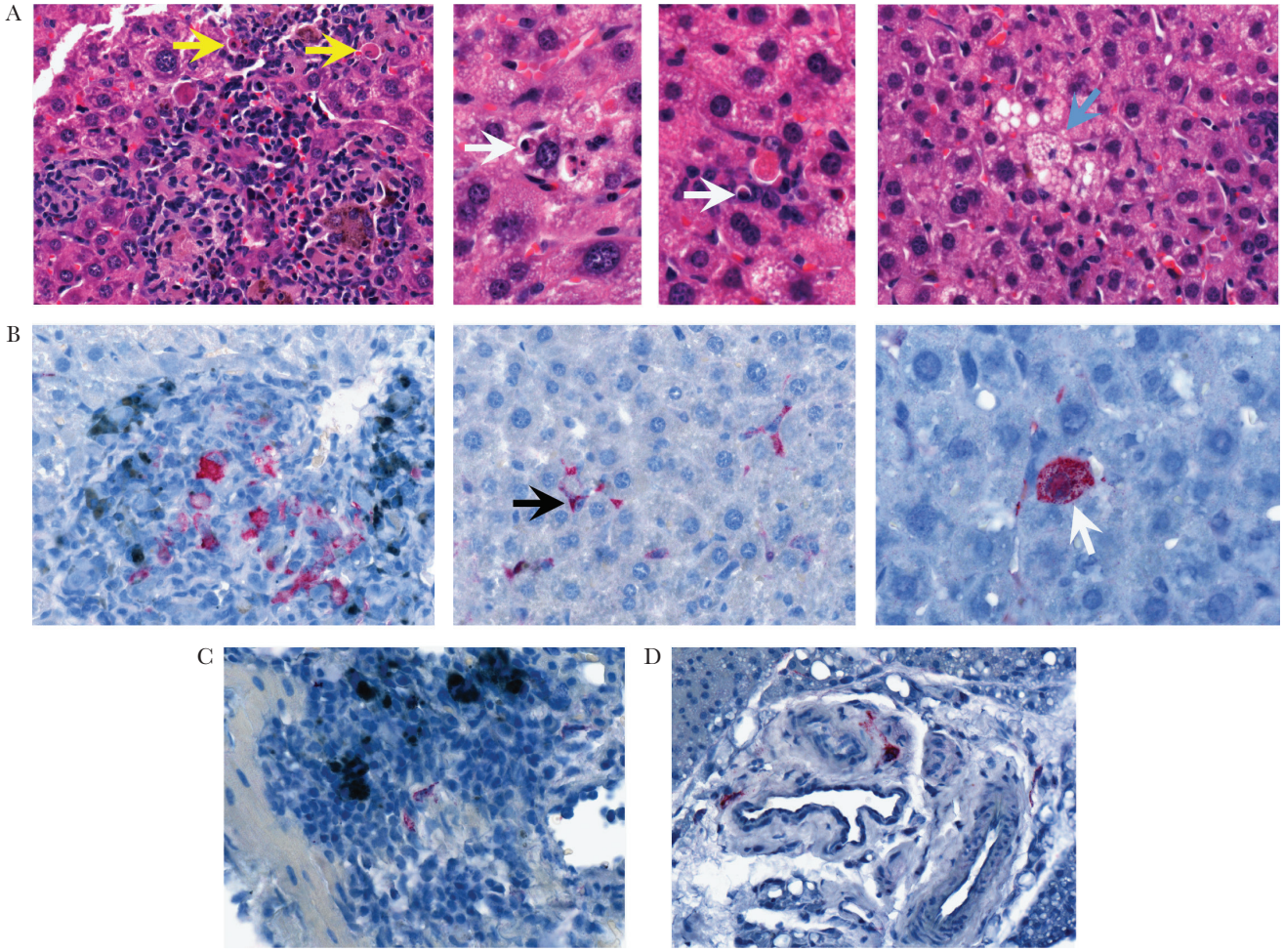


**Figure 3.** Extraneural histological analysis of humanized mice infected with Crimean-Congo hemorrhagic fever virus (CCHVF). Pulmonary, hepatic, and splenic findings described in control mice, including the presence of mixed inflammatory infiltrate, were also noted in CCHFV-infected humanized mice and considered secondary to factors outside the experimental viral infection. *A,* In contrast to control mice, an increase in individual hepatocellular death was observed both within the inflammatory foci (*yellow arrows*) and randomly throughout the parenchyma (*white arrows*). Vacuolar degeneration, indicating hepatocellular damage, was also noted in some animals (*blue arrow*). *B,* In the liver, with use of an anti-CCHFV antibody, immunoreactivity was seen in histiocytes and multinucleated giant macrophages within hepatic inflammatory foci (*left image*), Kupffer cells (*black arrow*), and rare hepatocytes (*white arrow*). *C, D,* Rare staining was also noted within mononuclear cells in the lung (*C*) and in mesenchymal connective tissue that remained adherent to organs when sampled at necropsy, such as perirenal adipose (*D*).

either CCHFV-OM or CCHFV-TR. High levels of viral RNA were detected in the brains of CCHFV-TR–infected animals that succumbed to disease, up to 2 logs higher than levels in CCHFV-OM animals at study completion. Ocular involvement is reported in other neurotropic viral infections. Thus, after virus was detected at high levels in brains of mice that succumbed to disease at 13 days after infection, ocular samples were collected for PCR analyses in the remaining mice (TR-5 and TR-6, n = 2; OM-4 through OM-9, n = 6); viral RNA was detected in all ocular samples from CCHFV-inoculated mice, regardless of strain.

#### CD45$^+$ Depletion and Differential T-Cell Activity and Function in CCHFV-Infected Humanized Mice

SGM3 humanized mice support high levels of human CD45$^+$ cell reconstitution, which may contribute to the immune response to viral infections [15–17]. hCD45$^+$ reconstitution levels were similar at 4 days after infection in mock-inoculated control mice and infected mice regardless of challenge virus (>60% engraftment; Figure 2A). However, in infected mice that were euthanized, either because of disease or at the scheduled end of the experiment, hCD45$^+$ levels were significantly lower than in controls, regardless of virus strain. This may represent apoptosis or direct infection of these cells by CCHFV or may be due to cellular localization to sites that were not sampled.

Both phenotypic activation on T cells and cytotoxic functional activity were assessed in the mice. Up-regulation of HLA-DR and CD38, markers of human T-cell activation [18, 19], was observed in all humanized mice infected with CCHFV, regardless of strain, sample time point, or disease outcome (Figure 2A). The early activation marker CD69 was also examined but was not notably elevated at any time point on either CD4$^+$ or CD8$^+$ T cells in infected mice compared with control mice (Supplementary

Figure S2). Of note, elevated levels of perforin, a marker of cytotoxic functional activity, were observed in the $CD8^+$ T cells of the mice that had to be euthanized after CCHFV-TR infection (Figure 2B). It is unclear whether this represents a population of $CD8^+$ T cells that could manage to nonspecifically kill infected cells in these animals or a population of $CD8^+$ T cells that were contributing to immune-mediated disease.

#### Histological and Immunohistochemical Evaluation of Extraneural Tissues in CCHFV-Infected SGM3 Humanized Mice

Hepatic cellular infiltrates, in both CCHFV-OM– and CCHFV-TR–infected humanized mice, were largely consistent with control humanized mice (Supplementary Figure S3); cellular infiltrates were mild to moderate in all but 1 animal (TR-1), in which infiltrates were abundant. However, in all evaluated CCHFV-TR mice and in OM-9, individual cell death was more frequent and both present within inflammatory foci and randomly distributed throughout the parenchyma (Figure 3A). In addition, vacuolar degeneration was noted in some animals, as well as a mild ductular reaction. In contrast, the remaining CCHFV-OM mice exhibited only rare, single-cell hepatocyte death associated with the inflammatory foci, similar to the control mice. Histopathological changes in lungs and spleens of infected humanized mice were consistent with those observed in control mice. Other tissues examined, including heart, eye, kidney, adrenal gland, and ovary/uterus, revealed no significant findings.

Immunohistochemistry for CCHFV showed staining in the liver, spleen, lungs, and adrenal glands (Table 1). In the liver, strong cytoplasmic immunoreactivity was noted primarily in histiocytes and multinucleated giant macrophages within inflammatory foci; sinusoidal lining cells, including Kupffer cells and endothelial cells; and in rare hepatocytes (Figure 3B). Immunoreactivity was noted within rare mononuclear cells consistent with histiocytes in the splenic white pulp (consistent with dendritic cells) and in perivascular inflammatory foci within the lungs (Figure 3C). Small numbers of mesenchymal cells in connective and adipose tissues that were adherent to organs were immunoreactive, including tissues surrounding organs in which immunostaining was not observed (kidney, eye, heart; Figure 3D), which may explain viral RNA detection by PCR in organs that were negative by immunohistochemistry. Finally, rare spindle cells consistent with endothelial cells had cytoplasmic staining in the adrenal gland of 2 animals (TR-4 and TR-6 at 20 and 23 days after infection, respectively).

#### Severe Neurological Disease in CCHFV-TR–Infected SGM3 Humanized Mice

Severe neurological disease and positive immunostaining for CCHFV were noted in the CCHFV-TR mice that were

**Table 1. Immunohistochemical Evaluation of Tissues with Anti-CCHFV Antibody[a]**

| Animal Designation | Time After Infection, d | Brain | Liver | Spleen | Lung | Ovary | Uterus | Kidney | Adrenal | Eye | Heart | GI Tract |
|---|---|---|---|---|---|---|---|---|---|---|---|---|
| DMEM-1 | 4 | – | – | – | NS | – | – | – | NS | NS | NS | NS |
| DMEM-2 | 33 | – | – | – | – | – | NS | – | NS | – | – | – |
| DMEM-3 | 33 | NS | – | – | – | – | – | – | – | – | – | – |
| DMEM-4 | 33 | – | – | – | – | – | NS | – | – | – | – | – |
| TR-1 | 4 | – | ++ | ++ | NS | NS | NS | – | – | NS | NS | NS |
| TR-2 | 4 | – | ++ | ++ | NS | NS | NS | – | – | NS | NS | NS |
| TR-3 | 4 | – | ++ | ++ | NS | NS | NS | – | – | NS | NS | NS |
| TR-4[b] | 20 | +++ | ++ | + | + | – | – | – | + | NS | – | – |
| TR-5[b] | 23 | +++ | + | NS | + | – | – | – | NS | – | – | – |
| TR-6[b] | 23 | +++ | ++ | ++ | + | – | – | – | + | – | – | – |
| TR-7[b] | 13 | +++ | ++ | + | + | NS | NS | – | – | NS | – | – |
| TR-8[b] | 13 | +++ | ++ | + | + | NS | NS | – | NS | NS | – | – |
| OM-1 | 4 | – | ++ | ++ | NS | NS | NS | – | – | NS | NS | NS |
| OM-2 | 4 | – | + | – | NS | NS | NS | – | – | NS | NS | NS |
| OM-3 | 4 | – | ++ | – | NS | NS | NS | – | – | NS | NS | NS |
| OM-4 | 33 | NS | NS | – | – | NS | – | – | NS | – | – | – |
| OM-5 | 33 | – | + | – | – | NS | NS | – | NS | – | – | – |
| OM-6 | 33 | – | + | – | – | – | – | – | – | – | – | – |
| OM-7 | 33 | – | – | NS | – | NS | NS | – | – | – | – | – |
| OM-8 | 33 | – | + | NS | + | NS | – | – | – | – | – | – |
| OM-9 | 33 | – | + | NS | – | NS | – | – | NS | – | – | – |

Abbreviations: –, negative results at staining; +, mild immunostaining; ++, moderate immunostaining; +++, abundant immunostaining; CCHFV, Crimean-Congo hemorrhagic fever virus; DMEM, Dulbecco's modified Eagle's medium; GI, gastrointestinal; NS, not sampled (ie, samples not obtained and/or not evaluated with immunohistochemistry).

[a]Tissues from SGM3 humanized mice inoculated with CCHFV isolated from a human patient in Turkey (CCHFV-TR) or Oman (CCHFV-OM) and euthanized at the indicated day after infection were stained with anti-CCHFV antibodies to detect the virus. Viral antigen was localized to brain, hepatic, splenic, and pulmonary tissues, with adrenal staining seen in a subset of CCHFV-TR mice. Antigen was most abundant in CCHFV-TR–inoculated mice euthanized because of disease.

[b]Euthanized because of disease.

euthanized owing to progressive weight loss at 13, 20, and 23 days after infection (Figure 4); no remarkable histological changes or anti-CCHFV immunohistochemistry immunoreactivity were seen in any CCHFV-inoculated mice euthanized at 4 days after infection, or in any CCHFV-OM survivors.

In CCHFV-TR mice with terminal-stage disease, patchy, mild to moderate expansion of the meninges by mixed but predominately mononuclear inflammatory cells composed of lymphocytes, including rare $CD8^+$ lymphocytes, histiocytes, plasma cells, and some neutrophils with immature band and ring forms, was observed (Figure 4A). In severe cases, small numbers of cells extended into the subjacent cortical parenchyma and were associated with edema and vascular congestion with increased leukocytes. Two animals had multiple loose aggregates of activated glial cells and microglia, resident macrophage cells in the brain, consistent with early glial nodules both within the cerebrum and cerebellum (Figure 4B). By thin-section electron microscopy, a virus particle with morphologically consistent with a bunyavirus was found in brain parenchyma directly below the meninges (Figure 4C).

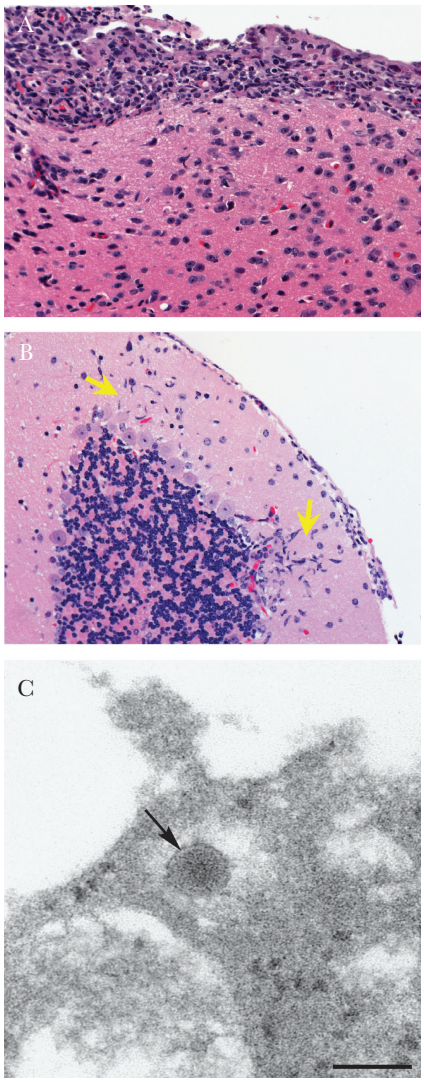


**Figure 4.** Disease in humanized mice with terminal-stage disease infected with a Crimean-Congo hemorrhagic fever virus strain isolated from a human patient in Turkey (CCHFV-TR) is associated with neurological disease. *A, B,* Mice euthanized because of weight loss all showed neuropathological changes consisting of a pleocellular meningitis (*A*) or meningoencephalitis, and gliosis with formation of glial nodules (*yellow arrows in B*). *C,* In 1 mouse, on-slide transmission electron microscopy from a region of intense immunostaining showed a bunyaviruslike particle (black arrow), 75 nm in diameter, with the characteristic homogenous inner core, then a space surrounded by an envelope (bar represents 100 nm).

Mild to extensive anti-CCHFV immunostaining was seen throughout the brains of CCHFV-TR humanized mice with terminal-stage disease, though comprehensive evaluation of all regions from every brain was not possible due to the nature of the samples. Immunostaining corresponded to regions of pathological changes observed with hematoxylin-eosin evaluation, and the most common pattern seen was abundant immunostaining in areas of meningitis/meningoencephalitis and within reactive astrocytes in areas of gliosis, with extension of immunostaining into the subpial food processes (Figure 5A). In 1 animal (TR-4, at 20 days after infection), multiple astrocytic foci were present in the cerebellar cortex, with cell bodies within the Purkinje layer, consistent with Bergmann glial cells (Figure 6A and 6B). In addition, widely dispersed rare immunostaining of glial cells and neurons was also present without notable neuropathological changes. This included both single glial and neuronal cells, and clusters of neurons localized to specific nuclei, such as the habenular nucleus (Figure 5A). Confirmation of these cells as astrocytes or neurons was accomplished by double staining against CCHFV and glial fibrillary acidic protein (Figures 5B, 5C, 6C, and 6D), and by cellular morphology.

## DISCUSSION

Pathogenesis studies of CCHF in animal models are limited because most vertebrate species other than humans, although susceptible to CCHFV infection [20], do not show signs of disease [21]. Even nonhuman primates, the reference standard animal model for other highly pathogenic hemorrhagic fever viruses that cause disease predominantly restricted to humans (eg, Ebola and Marburg viruses [22]), appear to be largely refractory to CCHF disease [23–26]. In this article, we describe a new lethal mouse model of CCHF, in SGM3 humanized mice, characterized by neurological disease and several liver histopathological features comparable to those in human cases, including vacuolar degeneration/steatosis, increased single-cell necrosis, and distribution of viral antigen within Kupffer cells, endothelial cells, and hepatocytes [27, 28].

In wild-type mice inoculated with CCHFV, viremia is either absent or mild and transient, and low levels of viral RNA are detected in an array of tissues without any clinical signs [9–11]. Virus is widely disseminated in humanized mice, similar to findings in $IFNAR^{-/-}$ and $STAT\text{-}1^{-/-}$ mice. However, the time from exposure until euthanasia criteria are met is more prolonged

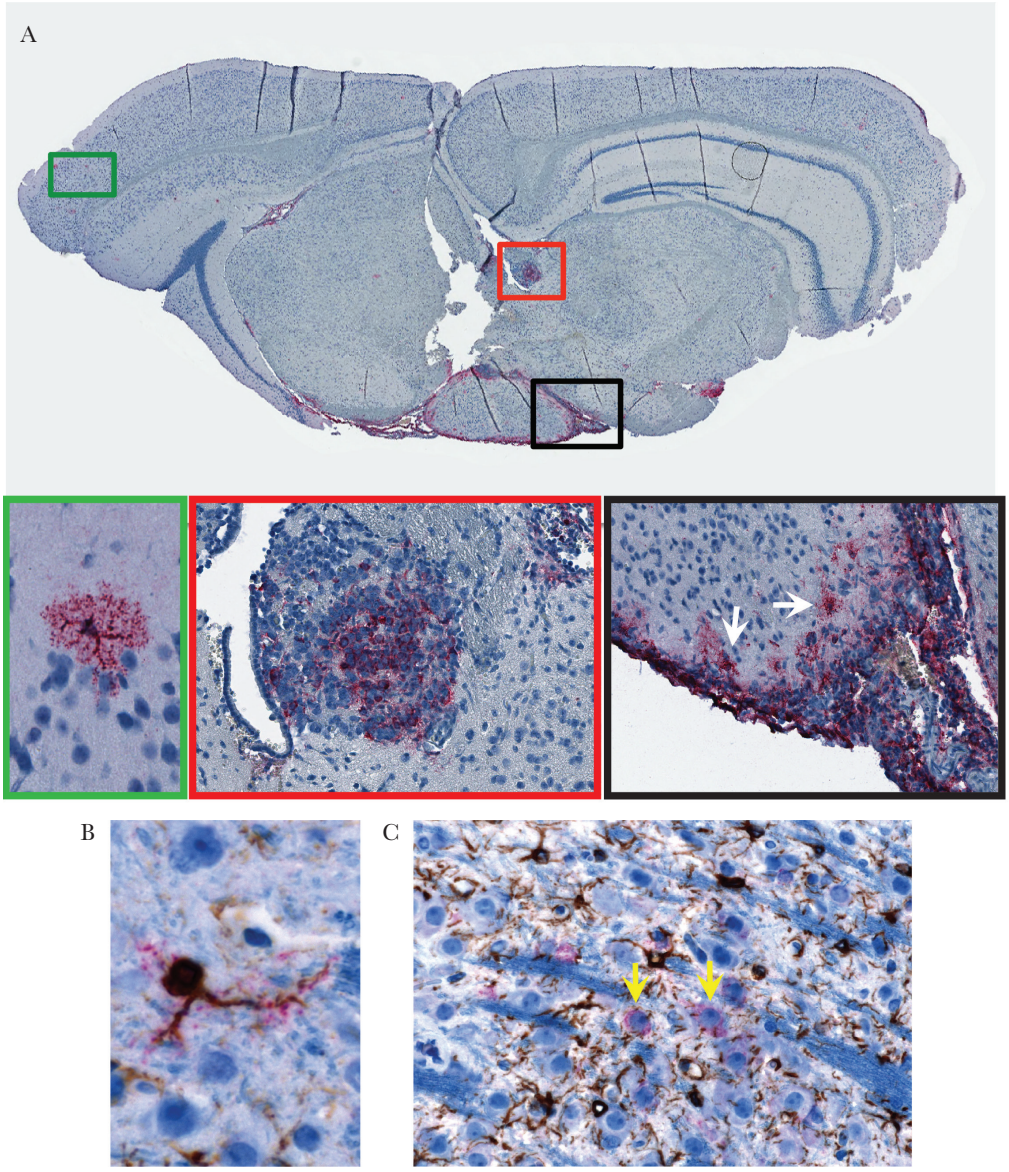


**Figure 5.** Infection of glial cells and neurons in humanized mice with terminal-stage disease infected with a Crimean-Congo hemorrhagic fever virus strain isolated from a human patient in Turkey (CCHFV-TR). Abundant anti-CCHFV immunostaining in glial cells and rare focal immunoreactivity in neurons were observed. *A,* Transverse section through the brain of a CCHFV-TR–infected mouse shows multiple foci of immunostaining for CCHF. Intense staining of neurons from the habenular nucleus is noted (*red box*). Immunostaining of the meninges and reactive astrocytes (*arrows in black box*) is seen in the hypothalamus. Strong, diffuse cytoplasmic immunoreactivity is seen in a reactive astrocyte (*green box*). *B,* Astrocytes show colocalization of glial fibrillary acidic protein (GFAP; *brown*) and CCHFV (*red*). *C,* Neurons with strong cytoplasmic immunoreactivity for CCHFV (*red, yellow arrows*) are surrounded by astrocytes and astrocytic cell processes that are immunoreactive with GFAP staining (*brown*).

than in existing immunodeficient mouse models of CCHF, and thus more consistent with the time course seen in fatal human cases (incubation of 1–13 days, and death generally after 5–14 days) [29]. Viral RNA was detected in the brains of humanized mice at 4 days after infection, increased over time, and had its highest levels in the brains of mice that succumbed to disease. In contrast, CCHFV is detected in the brains of IFNAR$^{-/-}$ and STAT-1$^{-/-}$ mice, but at lower levels than in other tissues (eg, liver and spleen) [9, 11]. This difference is probably due to the length of the clinical course in each model; the rapid, acute nature of disease in IFNAR$^{-/-}$ and STAT-1$^{-/-}$ mice (< 7 days) may prohibit high levels of viral dissemination into the brain, as seen in other models of viral infection when disease course is abbreviated rather than prolonged (eg, Nipah virus) [30].

In humanized mice, abundant CNS anti-CCHFV immunostaining was seen in the meninges and glia limitans, and in some regions submeningeal vessels were prominent, congested, and associated with parenchymal edema, indicators of vascular leakage. Endothelial damage is believed to be a central pathological mechanism in CCHF; increased levels of markers for

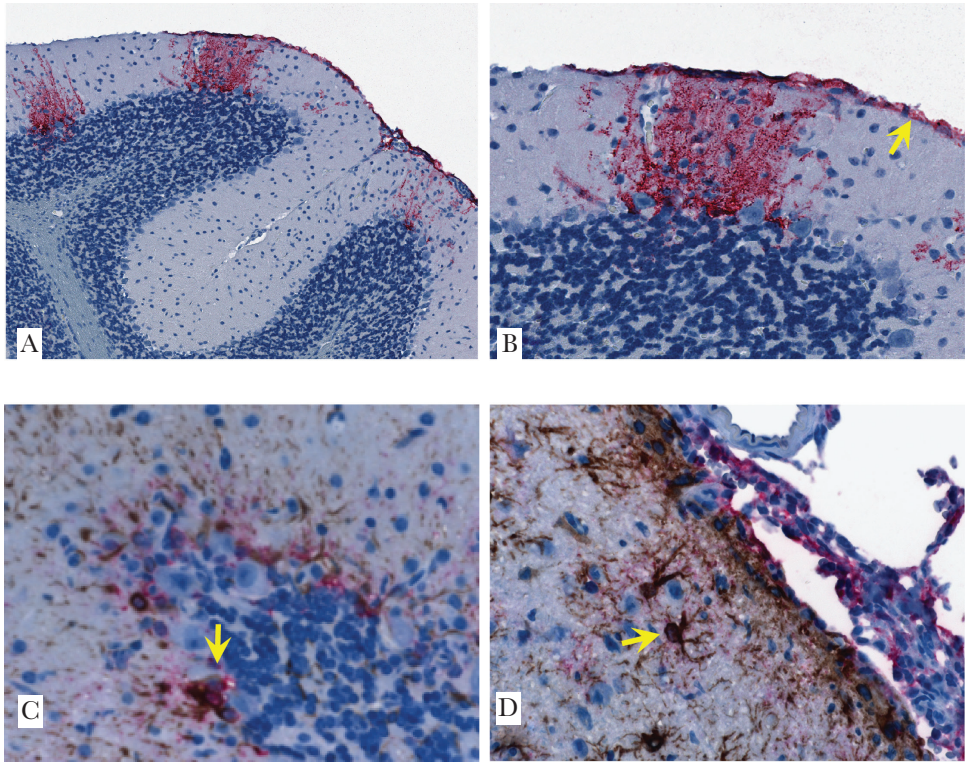


**Figure 6.** Astrocyte anti–Crimean-Congo hemorrhagic fever virus (CCHFV) immunoreactivity and gliosis in humanized mice with terminal-stage disease infected with a CCHFV strain isolated from a human patient in Turkey (CCHFV-TR). *A, B,* Multiple clusters of astrocytes with cell bodies adjacent to the Purkinje cells were present within the cerebellum in areas of gliosis noted histologically. Immunostaining extends into the subpial astrocytic processes (*arrow in B*). *C, D,* Infection of these cells is visualized by colocalization of glial fibrillary acidic protein (*brown*) and CCHFV (*red*) antigens (*arrows*).

endothelial and vascular damage, and plasma leakage are positively association with severity of disease [31]. As described in human cases, we detected CCHFV antigen in endothelial cells of several organs, including the liver and adrenal gland. These findings, including viral tropism for endothelial cells and histopathological evidence of vascular leakage in the brain, along with previous reports of vascular compromise, support hematogenous entry of CCHFV through a compromised blood-brain barrier (BBB) at the level of the brain microvessel endothelium.

Given the propensity for glial cell infection in the brains of the SGM3 humanized mice, CCHFV entry is probably enhanced by activation of astrocytes and impairment of their contribution to barrier function. Foot processes from astrocytes form a complex network surrounding the capillaries, and this close cell association is important in induction and maintenance of the barrier properties [32]. Glial cells form a structural framework to support neuronal cells and play a role in preventing pathogen entry into the brain. Morphological and functional BBB characteristics depend on the CNS environment and on the contribution of perivascular astrocytes [33, 34]. Furthermore, an astrocyte-mediated bystander effect has been described with other encephalitic viruses, in which infected astrocytes in an endothelial cell coculture model increased permeability of the endothelium, causing endothelial cell apoptosis, morphologically altered astrocytes, and gap junction–dependent disruptions in signaling between uninfected and infected cells [35]. Altogether, infection of glial cells and astrocytes provides a mechanism of disease consistent with reports of increased permeability in brain membranes of patients [2, 5].

The neurological involvement described in CCHF case reports may be primarily due to cytokine-mediated endothelial barrier dysfunction, or may be a direct effect of the virus in the brain [6]. Astrocytes may also play a role in disrupting CNS barriers in response to T-cell activation. $CD8^+$ T-cell activation of astrocytes is a well-described mechanism of BBB disruption [36, 37]. We were able to detect only rare human $CD8^+$ T cells in the brains of these mice by immunohistochemistry; however, it is unclear whether their presence, although in low numbers, directly contributes to alterations in CNS barriers or is secondary to disruption permitting cellular infiltration. Determining the role of these cells and characterizing CCHFV-mediated immune stimulation in the brain warrant future investigations.

We identified focal areas of immunoreactivity in the region of the habenular nuclei and in the hypothalamus (Figure 5A). Both of these regions are parts of the limbic system, a set of

brain structures that mediate a variety of emotional and motivational processes [38]. Infection of these regions is described in other neurotropic viral infections, including neurotropic influenza and a neurotropic murine coronavirus [39, 40]. Of particular interest is the hypothalamus because CCHFV has been isolated from the patient's hypothalamus in a fatal case [3]. In SGM3 humanized mice, we observed abundant CCHFV immunostaining of the hypothalamic meninges, and astrocytes in the presence of meningitis and reactive astrocytosis. The infection of these regions, seen in both human patients and humanized mice, suggests that future investigations should evaluate acute and long-term physiologic regulatory function and behavioral abnormalities in CCHF.

It is not unprecedented for a viral disease with overt hemorrhagic signs to also affect the brain. Lassa virus, Junin virus, and other hemorrhagic arenaviruses enter the brain and cause neurological symptoms that can include encephalitis, hearing loss, and tremors [41, 42]. Similar to our observations in CCHFV brain infection of SGM3 humanized mice, Junin virus also infects astrocytes, and neurodegenerative reactive astrogliosis may play a role in the pathogenesis of acute and late neurological symptoms in Junin virus infection [43–46]. Furthermore, many closely related bunyaviruses, including those of the California serogroup (genus *Orthobunyavirus*) and Rift Valley fever virus (genus *Phlebovirus*) are well characterized as causing neurological symptoms in human disease, supporting the potential for more frequent neurological involvement in CCHF than currently recognized.

Findings in recent cases and animal model studies of Ebola virus disease [47, 48] emphasize the need to consider viral dissemination to immune-privileged sites, such as the brain, even in viral disease not initially thought to have CNS involvement. CCHFV has demonstrated neurotropism in severe disease [3], but to our knowledge there have been no detailed investigations of CNS infection. Neither of the 2 reports of histopathological findings in human CCHF cases included findings in nervous tissue [27, 49], and CCHF research has been limited to severely immunocompromised mouse strains that develop rapid, acute disease prohibiting dissemination to the CNS. Although limitations remain in the use of humanized mouse models, these models have been instrumental in studies of human-specific viruses, bacteria, and parasites [50].

In this article, we present a novel humanized mouse model of CCHF, describing cellular targets and focal regions of infection in the brain. Our studies form a basis for more comprehensive research on (1) mechanisms of viral entry into the CNS, (2) neuroanatomical targets of infection, (3) viral persistence in the CNS, and (4) incidence of neurological signs and sequelae in human CCHF. Answers to these questions will be instrumental in determining the public health impact of CNS infection by CCHFV, guiding appropriate clinical care for patients, and developing targeted medical countermeasures.

## Supplementary Data

Supplementary materials are available at *The Journal of Infectious Diseases* online. Consisting of data provided by the authors to benefit the reader, the posted materials are not copyedited and are the sole responsibility of the authors, so questions or comments should be addressed to the corresponding author.

## Notes

***Acknowledgments.*** We thank Pierre Rollin for initial strain isolation studies, Lisa Guerrero and César Albariño for assistance with next generation sequencing, Silvia Sisó for neuropathology consultation, Tim Flietstra for guidance on statistical analyses, Tatyana Klimova for assistance with editing the manuscript, Stephen Welch and Joy Gary for assistance with figures, Jonathan Towner for critical review, and members of the CDC's Comparative Medicine Branch for providing care for the animals.

***Financial support.*** This work was partially supported by an appointment to the Research Participation Program at the CDC administered by the Oak Ridge Institute for Science and Education through an interagency agreement between the US Department of Energy and the CDC, by the National Institutes of Health (loan repayment award to J. R. S.), and by a CDC foundation project funded by the National Institute of Allergy and Infectious Diseases (grant R01AI109008 to E. B.).

***Potential conflicts of interest:*** All authors: No reported conflicts of interest. All authors have submitted the ICMJE Form for Disclosure of Potential Conflicts of Interest. Conflicts that the editors consider relevant to the content of the manuscript have been disclosed. The findings and conclusions in this report are those of the authors and do not necessarily represent the official position of the Centers for Disease Control and Prevention.

## References

1. Grashchenkov N. Investigations of etiology, pathogenesis, and clinical symptomatology of Crimean hemorrhagic fever [in Russian] (in English: NAMRU3-T1189). Reports 1944 Sci Investig Inst Neurol Akad Med Nauk SSSR; Moskva **1945**; 100–7.
2. Neklyudov M. A case of hemorrhagic fever (Crimea) [in Russian] (in English: NAMRU3-T1514). Suvrem Med Sof **1952**; 5:92–5.
3. Butenko A. Data from studying etiology, laboratory diagnosis, and immunology of Crimean hemorrhagic fever; questions of ecology of the viral agent [in Russian] (in English: NAMRU3-T1152). Inst Polio Virus Entsef, Akad Med Nauk SSSR Moskva **1971**.
4. Smorodintsev A, Kazbintsev L, Chudakov V. Virus hemorrhagic fevers [in Russian] (in English: Isreal Progam for Scientific Translations, Jerusalem). **1963**; 2–156.

5. Kleib AS, Salihy SM, Ghaber SM, Sidiel BW, Sidiya KC, Bettar ES. Crimean-Congo hemorrhagic fever with acute subdural use of plasma therapy for severe fever with thrombocytopenia syndrome encephalopathy. Emerg Infect Dis **2016**; 22:7–8.
6. Conger NG, Paolino KM, Osborn EC, et al. Health care response to CCHF in US soldier and nosocomial transmission to health care providers, Germany, 2009. Emerg Infect Dis **2015**; 21:23–31.
7. Chastel C. Erve and Eyach: two viruses isolated in France, neuropathogenic for man and widely distributed in Western Europe. Bull Acad Natl Med **1998**; 182:801-9-10.
8. Dilcher M, Koch A, Hasib L, Dobler G, Hufert FT, Weidmann M. Genetic characterization of Erve virus, a European Nairovirus distantly related to Crimean-Congo hemorrhagic fever virus. Virus Genes **2012**; 45:426–2.
9. Bente DA, Alimonti JB, Shieh WJ, et al. Pathogenesis and immune response of Crimean-Congo hemorrhagic fever virus in a STAT-1 knockout mouse model. J Virol **2010**; 84:11089–100.
10. Bereczky S, Lindegren G, Karlberg H, Akerström S, Klingström J, Mirazimi A. Crimean-Congo hemorrhagic fever virus infection is lethal for adult type I interferon receptor-knockout mice. J Gen Virol **2010**; 91:1473–7.
11. Zivcec M, Safronetz D, Scott D, Robertson S, Ebihara H, Feldmann H. Lethal Crimean-Congo hemorrhagic fever virus infection in interferon α/β receptor knockout mice is associated with high viral loads, proinflammatory responses, and coagulopathy. J Infect Dis **2013**; 207:1909–21.
12. National Research Council of the National Academies. Guide for the care and use of laboratory animals. 8th ed. Washington, DC: National Academy Press; **2011**.
13. Reed LJ, Muench H. A simple method for estimating fifty percent endpoints. Am J Hyg **1938**; 27:493–7.
14. Hayat M. Principles and techniques of electron microscopy: biological applications. 4th ed. Cambridge, UK, and New York, NY: Cambridge University Press; **2000**.
15. Billerbeck E, Barry WT, Mu K, Dorner M, Rice CM, Ploss A. Development of human $CD4^{+}FoxP3^{+}$ regulatory T cells in human stem cell factor-, granulocyte-macrophage colony-stimulating factor-, and interleukin-3-expressing NOD-SCID $IL2R\gamma^{null}$ humanized mice. Blood **2011**; 117:3076–86.
16. Spengler JR, Lavender KJ, Martellaro C, et al. Ebola virus replication and disease without immunopathology in mice expressing transgenes to support human myeloid and lymphoid cell engraftment. J Infect Dis **2016**; 214:308–18.
17. Wunderlich M, Chou FS, Link KA, et al. AML xenograft efficiency is significantly improved in NOD/SCID-IL2RG mice constitutively expressing human SCF, GM-CSF and IL-3. Leukemia **2010**; 24:1785–8.
18. Long BR, Stoddart CA. Alpha interferon and HIV infection cause activation of human T cells in NSG-BLT mice. J Virol **2012**; 86:3327–36.
19. Shultz LD, Saito Y, Najima Y, et al. Generation of functional human T-cell subsets with HLA-restricted immune responses in HLA class I expressing NOD/SCID/IL2r gamma(null) humanized mice. Proc Natl Acad Sci U S A **2010**; 107:13022–7.
20. Spengler JR, Bergeron É, Rollin PE. Seroepidemiological studies of Crimean-Congo hemorrhagic fever virus in domestic and wild animals. PLoS Negl Trop Dis **2016**; 10:e0004210.
21. Spengler JR, Estrada-Peña A, Garrison AR, et al. A chronological review of experimental infection studies of the role of wild animals and livestock in the maintenance and transmission of Crimean-Congo hemorrhagic fever virus. Antiviral Res **2016**; 135:31–47.
22. Geisbert TW, Strong JE, Feldmann H. Considerations in the use of nonhuman primate models of Ebola virus and Marburg virus infection. J Infect Dis **2015**; 1–7.
23. Butenko A, Chumakov M, Smirnova S, et al. Isolation of CHF virus from blood of patients and corpse material (from 1968–1969 investigation data) in Rostov and Astrakhan oblasts, and Bulgaria [in Russian] (in English: NAMRU3-T522). Mater 3 Obl Nauchn Prakt Konf **1970**; 6–25.
24. Fagbami AH, Tomori O, Fabiyi A, Isoun TT. Experimental Congo virus (Ib-AN 7620) infection in primates. Virologie **1975**; 26:33–7.
25. Smirnova SE. A comparative study of the Crimean hemorrhagic fever-Congo group of viruses. Arch Virol **1979**; 62:137–43.
26. Alimonti J, Leung A, Jones S, et al. Evaluation of transmission risks associated with in vivo replication of several high containment pathogens in a biosafety level 4 laboratory. Sci Rep **2014**; 4:5824.
27. Joubert JR, King JB, Rossouw DJ, Cooper R. A nosocomial outbreak of Crimean-Congo haemorrhagic fever at Tygerberg Hospital. III. Clinical pathology and pathogenesis. S Afr Med J **1985**; 68:722–8.
28. Burt FJ, Swanepoel R, Shieh WJ, et al. Immunohistochemical and in situ localization of Crimean-Congo hemorrhagic fever (CCHF) virus in human tissues and implications for CCHF pathogenesis. Arch Pathol Lab Med **1997**; 121:839–46.
29. Bente DA, Forrester NL, Watts DM, McAuley AJ, Whitehouse CA, Bray M. Crimean-Congo hemorrhagic fever: history, epidemiology, pathogenesis, clinical syndrome and genetic diversity. Antiviral Res **2013**; 100:159–89.

30. Rockx B, Brining D, Kramer J, et al. Clinical outcome of henipavirus infection in hamsters is determined by the route and dose of infection. J Virol **2011**; 85:7658–71.
31. Ozturk B, Kuscu F, Tutuncu E, Sencan I, Gurbuz Y, Tuzun H. Evaluation of the association of serum levels of hyaluronic acid, sICAM-1, sVCAM-1, and VEGF-A with mortality and prognosis in patients with Crimean-Congo hemorrhagic fever. J Clin Virol **2010**; 47:115–9.
32. Abbott NJ, Patabendige AA, Dolman DE, Yusof SR, Begley DJ. Structure and function of the blood-brain barrier. Neurobiol Dis **2010**; 37:13–25.
33. Janzer RC, Raff MC. Astrocytes induce blood–brain barrier properties in endothelial cells. Nature **1987**; 325:253–57.
34. Tao-Cheng JH, Nagy Z, Brightman MW. Tight junctions of brain endothelium in vitro are enhanced by astroglia. J Neurosci **1987**; 7:3293–9.
35. Eugenin EA, Clements JE, Zink MC, Berman JW. Human immunodeficiency virus infection of human astrocytes disrupts blood-brain barrier integrity by a gap junction-dependent mechanism. J Neurosci **2011**; 31:9456–65.
36. Johnson HL, Chen Y, Jin F, et al. CD8 T cell-initiated blood-brain barrier disruption is independent of neutrophil support. J Immunol **2012**; 189:1937–45.
37. Johnson HL, Willenbring RC, Jin F, et al. Perforin competent CD8 T cells are sufficient to cause immune-mediated blood-brain barrier disruption. PLoS One. **2014**; 9:4–11.
38. Morgane PJ, Galler JR, Mokler DJ. A review of systems and networks of the limbic forebrain/limbic midbrain. Prog Neurobiol **2005**; 75:143–60.
39. Mori I, Diehl AD, Chauhan A, Ljunggren HG, Kristensson K. Selective targeting of habenular, thalamic midline and monoaminergic brainstem neurons by neurotropic influenza A virus in mice. J Neurovirol **1999**; 5:355–62.
40. Sun N, Perlman S. Spread of a neurotropic coronavirus to spinal cord white matter via neurons and astrocytes. J Virol **1995**; 69:633–41.
41. Cummins D, Bennett D, Fisher-Hoch SP, Farrar B, Machin SJ, McCormick JB. Lassa fever encephalopathy: clinical and laboratory findings. J Trop Med Hyg **1992**; 95:197–201.
42. Wilson MR, Peters CJ. Diseases of the central nervous system caused by lymphocytic choriomeningitis virus and other arenaviruses. Handb Clin Neurol **2014**; 123:671–81.
43. Berría MI, Lascano EF. Astrocyte differentiation induced by Junín virus in rat brain cell cultures. Acta Neuropathol **1985**; 66:233–8.
44. Iacono RF, Nessi de Aviñón A, Rosetti FA, Berría MI. Glial fibrillary acidic protein (GFAP) immunochemical profile after Junin virus infection of rat cultured astrocytes. Neurosci Lett **1995**; 200:175–8.
45. Pozner RG, Collado S, Jaquenod de Giusti C, et al. Astrocyte response to Junín virus infection. Neurosci Lett **2008**; 445:31–5.
46. Kolokoltsova OA, Yun NE, Paessler S. Reactive astrogliosis in response to hemorrhagic fever virus: microarray profile of Junin virus-infected human astrocytes. Virol J **2014**; 11:126.
47. Howlett P, Brown C, Helderman T, et al. Ebola virus disease complicated by late-onset encephalitis and polyarthritis, Sierra Leone. Emerg Infect Dis **2016**; 22:150–2.
48. Scott JT, Sesay FR, Massaquoi TA, Idriss BR, Sahr F, Semple MG. Post-Ebola syndrome, Sierra Leone. Emerg Infect Dis **2016**; 22:641–6.
49. Burt FJ, Swanepoel R, Braack LE. Enzyme-linked immunosorbent assays for the detection of antibody to Crimean-Congo haemorrhagic fever virus in the sera of livestock and wild vertebrates. Epidemiol Infect **1993**; 111:547–57.
50. Ernst W. Humanized mice in infectious diseases. Comp Immunol Microbiol Infect Dis **2016**; 49:29–38.